SESSION C:

HARDNESS

ASSURANCE

IEEE Transactions on Nuclear Science, Vol. NS-33, No. 6, December 1986

THE RELATIONSHIP BETWEEN ^{60}Co AND10-keV X-RAY DAMAGE IN MOS DEVICES

J. M. Benedetto and H. E. Boesch, Jr.
U.S. Army Laboratory Command
Harry Diamond Laboratories
Adelphi, Maryland 20783-1197

Abstract

This paper presents a conduction current technique to separate the effects of fractional charge yield and dose enhancement in metal-oxide semiconductor (MOS) devices in a 10-keV x-ray environment. The results of the conduction current measurements, together with the concept of charge generation as the damage-producing agent, are used to correlate the threshold-voltage shifts in gate- and field-oxide MOS field-effect transistors irradiated with ^{60}Co and a 10-keV x-ray machine. A straightforward procedure for calculating the equal-damage dose equivalence between the 10-keV x-ray and ^{60}Co sources is also presented.

1. Introduction

The interest in using low-energy x-ray sources for device testing and qualification continues to increase. The advantages of low-energy x-ray sources for testing parts at the wafer level are considerable compared to the traditional ^{60}Co source. However, a drawback to the general use of low-energy sources is the presence of significant edge effects (interface dose enhancement) in thin structures and altered charge yield per unit dose with respect to higher energy sources (e.g., ^{60}Co). These effects have been documented by Dozier and Brown [1-4] and Oldham and McGarrity [5].

In order to sort out these effects in a useful way and properly correlate low-energy x-rays to high-energy sources, we need to (1) identify a quantity that results from the radiation (that is, the primary agent causing radiation-induced damage in devices, and the effects of which are independent of the characteristics of the radiation source), and (2) relate this quantity to the specific characteristics of the radiation sources.

In the present work, we propose oxide charge generation (radiation generated charge per cubic centimeter) as the appropriate damage agent for metal-oxide semiconductor (MOS) devices and other oxide-related damage. Charge generation is the radiation generated charge per cubic centimeter in the oxide after initial electron-hole pair (EHP) recombination. We analyze charge generation in terms of the charge generation per unit dose component and the "true dose" component (bulk oxide dose times interface dose enhancement). We then present results of conduction current measurements that unambigously separate and quantify charge yield (the fraction of EHP's escaping initial recombination) and dose enhancement effects in the 10-keV x-ray source. Next, we demonstrate, with data taken on representative MOS devices, that the charge generation approach, together with the charge-yield and dose-enhancement results, successfully correlates x-ray and ^{60}Co gamma radiation-induced threshold-voltage-shift damage measured in both gate- and field-oxide devices. Finally, we present a straightforward procedure for calculating the equal-damage dose equivalence between the 10-keV x-ray and ^{60}Co sources.

2. Charge Generation and Radiation-Induced Damage in MOS Devices

The primary damage effect of ionizing radiation in MOS devices is threshold-voltage shift, ΔV_t, which is the sum of components due to trapping of radiation-generated holes in the oxide, ΔV_{ot}, and the radiation-induced buildup of interface states, ΔV_{it}. In the low-dose (linear) region, the hole-trapping damage component under positive bias is given by the expression

$$\Delta V_{ot} = \left[-t_{ox}^2 f_T(\varepsilon)/\varepsilon_i\right]\left[\rho_R(\varepsilon,E)\right] \quad , \tag{1}$$

where ε is the electric field in the oxide, E is the energy of the ionizing radiation source, t_{ox} is the oxide thickness, f_T is the fraction of holes trapped in the oxide near the Si/SiO_2 interface, and ε_i is the oxide dielectric constant. ρ_R is the radiation-generated charge density (in C/cm^3), or charge generation, in the oxide and is given by

$$\rho_R = \left[K_g(E)f_y(\varepsilon,E)\right]\left[R_{de}(E,t_{ox})D_o(E)\right] \quad , \tag{2}$$

where K_g is the charge generation constant (in $C/cm^3rad(SiO_2)$), f_y is the fractional radiation-generated charge yield, R_{de} is the dose enhancement factor, and D_o is the bulk or equilibrium oxide dose (in the absence of dose enhancement). The product of bulk dose times dose enhancement constitutes the "true dose" in the SiO_2 layer. The quantities in the left square brackets, the charge generation constant times the field-dependent fractional charge yield, give the radiation-generated charge in the oxide per unit dose (after initial recombination). The terms in the left-hand square brackets in Eq. (1) include device-processing and geometry-dependent quantities that relate ΔV_{ot} to ρ_R. The fraction of free holes that are trapped at the $Si\text{-}SiO_2$ interface has been found to be a function of electric field in the oxide [4,6], but is not apparently a function of ionizing radiation energy [4]. Note that ρ_R contains all the factors that are dependent on the energy of the radiation source and its output, while the geometry term is independent of the source. It should also be noted that most models of radiation-induced interface state production assume that the initial process is the generation of free charge in the oxide [7-9]. Therefore, we expect ΔV_{it} and mobility degradation to also be relatable to ρ_R, although probably in a much more complex manner than ΔV_{ot}. Thus, the radiation-generated charge density, or charge generation, meets the requirements for the primary damage agent that we wish to find.

3. Analysis of the Components of Charge Generation

We now examine the terms that contribute to ρ_R in more detail. As shown explicitly in Eq. (2), the yield of free EHP's has been found to be a function of the energy of the ionizing radiation delivering the dose, E [4], and the electric field, ε, in the oxide layer [2,5]. The effective dose enhancement factor depends on the nature and spectrum of the ionizing radiation and the oxide thickness. The bulk dose is the number generally calculated for the material as simply "dose," taking into account the energy and the linear energy transfer (LET) of the ionizing irradiation. Evidently, in the general case the charge generation (and, hence, the threshold shift and other effects) obtained in equivalent MOS devices will not

U.S. Government work not protected by U.S. Copyright.

be the same for different photon energy sources even if the nominal or bulk material dose, D_o, delivered to the samples is the same. Dozier and Brown [2] and Oldham and McGarrity [5], in work employing correlations between measurements using ^{60}Co gammas and low-energy x rays, have shown that the yield of EHP's from 10-keV photons can be a factor of two lower than that for 1.25-MeV photons at low fields. At high fields the photon energy becomes less of a factor, as most of the charge pairs are separated by the applied field before recombination occurs. Little dose enhancement occurs in the oxide near the polysilicon-SiO_2 or SiO_2-Si interfaces for 1.25-MeV photons, whereas a substantial flux of photoelectrons is expected from the polysilicon or silicon into the SiO_2 for 10-keV photons. For oxide thicknesses comparable to the photoelectron range (t_{ox} < 100 nm), R_{de}(10 keV)/R_{de}(1.25 MeV) is expected to be about 1.7 [10]. The net result is that substantial differences could be expected between low- and high-energy-photon irradiations of MOS devices.

3.1 Conduction Current Measurements

In order to correctly calculate charge generation in devices for different sources, we must have reliable values for the charge generation constant, fractional charge yield, and dose enhancement terms. In most measurements, K_g, f_y, and R_{de} cannot be separated without making some assumptions about one or the other. We applied a photocurrent measurement technique in order to measure these quantities and separate them in an unambiguous manner.

If a bias is applied across an MOS sample and the sample is irradiated, the radiation-generated EHP's created in the oxide give rise to a conduction current through the oxide. This current is proportional to oxide thickness and the rate of charge generation, $\dot{\rho}_R$, and is given by the expression

$$I_c = At_{ox}\dot{\rho}_R = At_{ox}\left[K_g(E)f_y(\varepsilon,E)R_{de}(E,t_{ox})\dot{D}_o\right] , \qquad (3)$$

where A is the electrode area and $\dot{D}_o$ is the bulk oxide dose rate.

The conduction current measurements to determine the fractional charge yield and interface dose enhancement for low-energy x rays were performed with an ARACOR model 4100 10-keV x-ray machine. The x-ray machine was fitted with a special sample holder that was designed to minimize stray radiation-induced currents by tightly collimating the x-ray beam so that only the active area of the chip received direct x-ray illumination. The sample holder was evacuable to a pressure of less than 10^{-5} Torr to eliminate air ionization effects. Attenuation of the x-ray beam was kept to a minimum by using a 0.5-mil Al window directly over the sample. Dosimetry for the sample holder in the x-ray machine was performed with a silicon p-i-n diode; the 0.5-mil Al window was in place during dosimetry.

The samples used for the conduction current measurements were supplied by Hughes Aircraft Corporation (HAC) and the Harry Diamond Laboratories (HDL) Microelectronics Facility. The HAC samples were nominal 25-mil dot Al-gate capacitors with oxide thicknesses from 22 to 98 nm. The samples from HDL were 80-mil/side square Al-gate capacitors with oxide thicknesses from 200 to 800 nm. The capacitors were fabricated without a field oxide, thereby avoiding stray current components from electrode areas overlapping the field oxide. The total dose received by the samples was sufficiently low (0.5 to 1.0 krad(SiO_2)) to avoid perturbing the oxide electric field. Each sample was irradiated with oxide fields ranging from 0.01 to 6 MV/cm. Above 6 MV/cm, Fowler-Nordheim injection currents began to overwhelm the conduction currents.

Figure 1 shows the conduction current versus oxide field for a 423-nm sample irradiated at a dose rate of 10^4 rad(SiO_2)/s (uncorrected for dose enhancement). Similar conduction current curves were generated for the other oxide samples. For all the samples tested the background currents were very small, on the order of 10^{-13} A (below 6 MV/cm). Figure 2 shows the current versus oxide field data replotted as reciprocal charge generation per unit dose versus reciprocal oxide field, the functional form predicted by the columnar recombination model [11]. The charge generation per unit dose is simply the conduction current normalized to oxide volume (At_{ox}) and dose rate (Eq. (3)). The normalization permits comparison of results from different samples and dose rates. For clarity, this figure shows the results of only four of the seven different sample types (the data for the thinner samples are essentially coincident with the 22.4-nm results). Extrapolating these curves to infinite field (zero abscissa) gives the infinite field, or maximum charge generation, value for each sample. Note that the slopes as well as the magnitudes of the curves for the various samples vary in an apparently nonsystematic way (in particular, the 423-nm points lie above the 766-nm points). This result is an effect of hole trapping in the bulk of the oxide layer which is dependent upon oxide processing and was observed in the thicker oxides (t_{ox} > 100 nm) [6]. Hole trapping in the oxide bulk has the effect of reducing the radiation-generated current by shortening the mean distance that the holes travel in the oxide after their generation. (Hole trapping at the Si/SiO_2 interface does not affect the current.) Since bulk hole trapping in these thick oxides varies as $\varepsilon^{-1/2}$ [6], it acts to preferentially decrease the measured current at low fields. Thus, the 423-nm sample, which showed the most bulk hole trapping, showed the largest slope in Fig. 2. It is crucial to note that, since bulk hole trapping varies as $\varepsilon^{-1/2}$, it goes to zero at infinite field and does not significantly affect the zero intercept (infinite field) values for the reciprocal of charge generation obtained in Fig. 2. The values for the maximum charge generation will be important for determining the fractional yield versus field and dose enhancement characteristics for the 10-keV x-ray source.

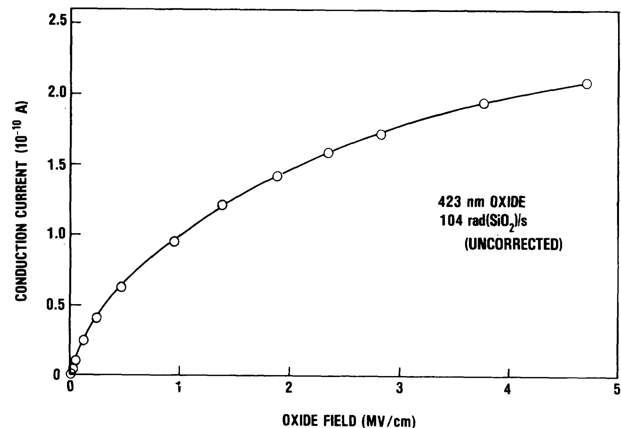

Figure 1. Conduction current versus oxide field for a 423-nm oxide sample irradiation with 10-keV x rays. Dose rate of 10^4 rad(SiO_2)/s is uncorrected for dose enhancement.

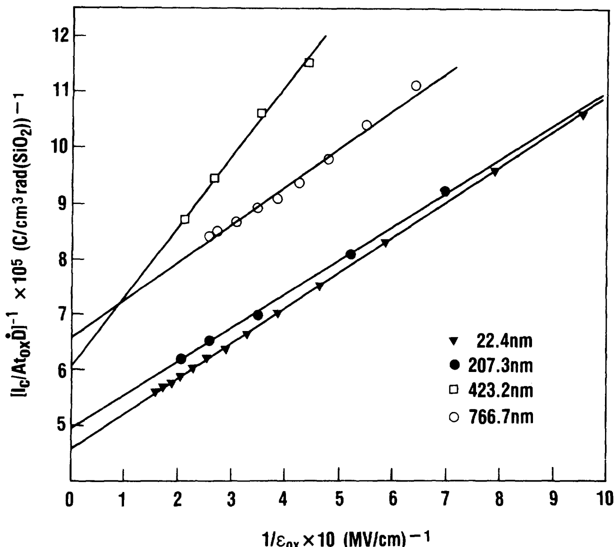

Figure 2. Conduction current normalized to oxide volume and dose rate versus reciprocal oxide field for four different oxide thicknesses. Data are extrapolated to $1/\varepsilon_{ox} = 0$ to generate the maximum charge generation values. Charge generation is normalized to oxide volume and bulk dose, but not dose enhancement.

The dose enhancement factor varies roughly inversely with oxide thickness for thicknesses above ~100 nm [5]. With this in mind, we plotted the maximum charge generation values obtained by the procedure described above for the three thickest samples as a function of reciprocal oxide thickness. A reasonable linear fit was obtained (Fig. 3). Extrapolating these data to infinite thickness then gives the maximum charge generation without dose enhancement (since $R_{de} \to 0$ as $t_{ox} \to \infty$). This quantity is simply $K_g^{x\text{-}ray}$, which is found to be $(1.38 \pm 0.14) \times 10^{-6}$ C/cm^{3}rad(SiO$_2$). Dividing each of these intercepts by $K_g^{x\text{-}ray}$ gives the dose enhancement, R_{de}, at each thickness. Figure 4 shows a plot of R_{de} versus oxide thickness for the data in this work (solid circles), the data of Oldham and McGarrity [5] (open circles), and theoretical calculations from Dozier and Brown [4] and Brown [12] (dashed lines). The data of Oldham and McGarrity were originally normalized to a maximum R_{de} of 1.7 from Dozier and Brown theory [4]; their data were renormalized to a maximum R_{de} of 1.6 before being plotted in Fig. 4. The agreement between the two sets of data is quite good. The Dozier and Brown calculation [4] agrees well for thin oxides, but departs from the data for thicknesses above 200 nm. The Brown calculations [12] agree well for thicker oxides. The data from this work, the data of Oldham and McGarrity [5], and the calculations of Dozier and Brown [4] give the dose enhancement versus oxide thickness for Al-gate devices. The calculations of Brown [12] are for polysilicon gate devices. Brown expects the dose enhancement versus oxide thickness to vary by approximately 10 percent between Al-gate and polysilicon gate devices [13].

Figure 5 is a plot of the fractional charge yield versus oxide field. The fractional charge yield is found by normalizing the charge generation by $K_g^{x\text{-}ray}$. The resulting values for f_y are lower than traditional values because the value obtained for $K_g^{x\text{-}ray}$ by extrapolation to infinite field is larger than its traditional value. Previous values for f_y (maximum) have been based on 100-percent hole yield at 3 to 4 MV/cm, giving $K_g = (1.2 \pm 0.15) \times 10^{-6}$ C/cm^{3}rad(SiO$_2$) [5,10]. Also shown in the figure are the data from Oldham and McGarrity [5] for yield as obtained from charge buildup measurements at 77 K

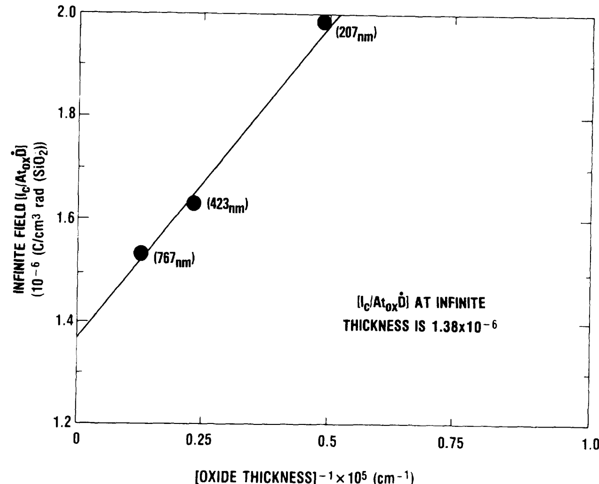

Figure 3. Infinite field normalized conduction current for 207-, 423-, and 767-nm samples plotted versus reciprocal oxide thickness. Data are extrapolated to infinite thickness ($1/t_{ox} = 0$) to determine the maximum charge generation independently of dose enhancement (since $R_{de} \to 0$ as $t_{ox} \to \infty$).

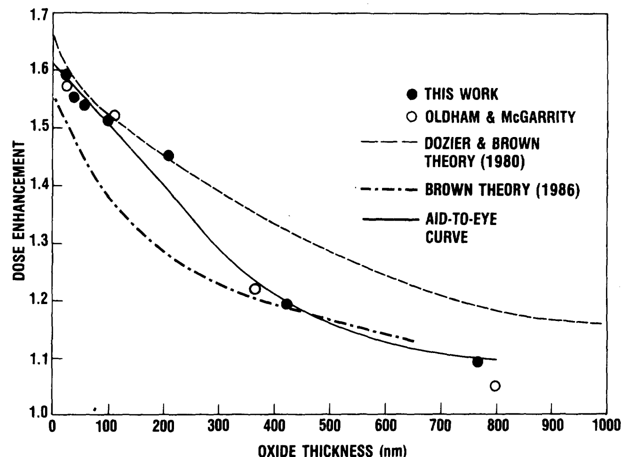

Figure 4. Dose enhancement versus oxide thickness. Solid circles represent data from this work; open circles are from Oldham and McGarrity [5]; dashed line is Dozier and Brown theory [4]; and dot-dash line is Brown theory [12].

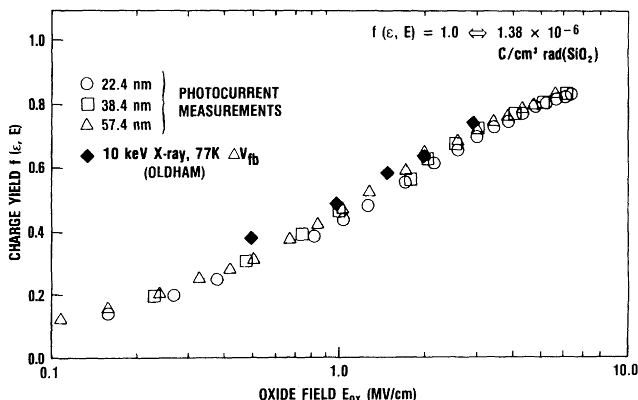

Figure 5. Charge yield plotted versus oxide field. Open symbols are data from this work; solid diamonds are from Oldham and McGarrity [5].

(solid diamonds). These data were renormalized to the new value for $K_g^{x\text{-}ray}$, and are in good agreement with the photocurrent results. A useful fit to the charge yield data (including a 77-K point at zero field) is given by the empirical expression

$$f_y^{x\text{-}ray}(\varepsilon) = [1.30/(\varepsilon + 0.113) + 1]^{-1} \quad , \qquad (4)$$

where ε here is the magnitude of the oxide field and is expressed in megavolts per centimeter.

The "traditional" value of 1.2×10^{-6} $C/cm^3rad(SiO_2)$ for K_g^{Co-60} and its accompanying values for $f_y^{Co-60}(\varepsilon)$ were based on measurements of hole yield in MOS capacitors at 77 K using a 13-MeV electron beam from a LINAC [14] and ^{60}Co photons [5]. In reality, K_g^{Co-60} is K_g^{LINAC}. The two measurements yielded essentially identical results for K_g^{LINAC}, K_g^{Co-60} and for $f_y^{LINAC}(\varepsilon)$, $f_y^{Co-60}(\varepsilon)$, since the ~1-MeV photons and 13-MeV electrons both produce widely scattered EHP's in the SiO_2 from high-energy secondary electrons. K_g^{LINAC} was calculated from the charge yield measured at 4 MV/cm--the maximum practical field for the 77 K experiment [14]--and was not, therefore, a true infinite field value. For present purposes, the high-field results for charge yield from the 77 K LINAC experiment were replotted as $1/f_y^{LINAC}(\varepsilon)$ versus $1/\varepsilon$ and extrapolated to infinite field (zero $1/\varepsilon$ intercept) as for the 10-keV x-ray current measurements discussed above. This procedure, as expected, produced a somewhat higher value for K_g^{LINAC} of $(1.3 \pm 0.15) \times 10^{-6}$ $C/cm3/rad(SiO2)$ and a correspondingly reduced set of values for f_y^{LINAC}.

In principle, the infinite-field charge yield per unit dose in SiO_2 should be independent of radiation source since the fundamental EHP generation process is initial energy-insensitive, and early electron-hole recombination is suppressed as the field is increased [11]. Therefore it is not surprising that, within experimental error, the values found for K_g^{Co-60} and $K_g^{x\text{-}ray}$ are essentially equal.

In parallel with the 10-keV x-ray results given above, a useful fit to the high-energy charge yield data is given by the expression

$$f_y^{Co-60}(\varepsilon) = f_y^{LINAC}(\varepsilon) = [0.27/(\varepsilon + 0.084) + 1]^{-1} \quad , \qquad (5)$$

where ε here is again the magnitude of the oxide field expressed in megavolts per centimeter. The fractional hole yield versus oxide thickness for the 10-keV x-ray source and ^{60}Co is shown in Fig. 6.

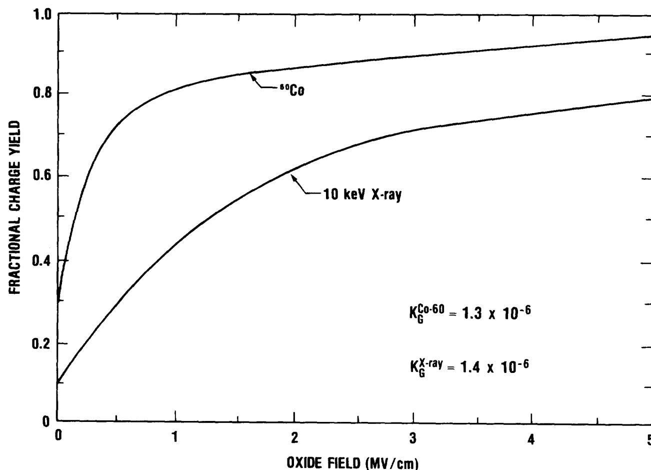

Figure 6. Charge yield versus oxide field for ^{60}Co and 10-keV x ray. The ^{60}Co and x-ray curves are based on a charge generation constant of 1.3×10^{-6} and 1.4×10^{-6} $C/cm^3rad(SiO_2)$, respectively.

To summarize the present results, we have measured and separated $K_g^{x\text{-}ray}$, $f_y^{x\text{-}ray}$, and $R_{de}^{x\text{-}ray}$ by using a photocurrent measurement technique and by taking advantage of the limiting characteristics of $f_y^{x\text{-}ray}$ and R_{de} as a function of field and oxide thickness, respectively. We have also recalculated values for K_g^{Co-60} and f_y^{Co-60} in a manner consistent with the x-ray results.

3.2 Threshold Voltage Correlation

In the previous section, results were obtained for dose enhancement and fractional charge yield in a 10-keV x-ray environment. This section uses these results to correctly calculate the charge generation, ρ_R, in the two sources (^{60}Co and 10-keV x rays) and thereby correlate the threshold voltage shift for gate- and field-oxide MOSFET's irradiated with ^{60}Co and 10-keV x rays. The MOSFET's used for the threshold correlation were supplied by four different DoD contractors. The MOSFET's consisted of both gate- and field-oxide devices. The gate-oxide transistors had a thickness range of 40 to 70 nm, and the field-oxide transistors had a thickness range of 500 to 700 nm, depending on the contractor. The gate-oxide devices were irradiated with a 1.25-MV/cm gate-to-source field, with the drain, source, and substrate all tied to ground. The field-oxide devices were irradiated with fields of approximately 0.1 and 0.5 MV/cm. Similarly, the drain, source, and substrate were held at ground.

The MOSFET's were irradiated in the ARACOR 10-keV x-ray tester and the HDL water-shielded ^{60}Co source. The dose rate for the ARACOR was determined from a calibrated Si p-i-n diode. The bulk dose rate in $rad(SiO_2)$ was obtained by dividing the dose rate in rad(Si) by 1.8 [15]. The HDL ^{60}Co source intensity was calibrated in roentgens through the National Bureau of Standards (NBS). The dose rate in $rad(SiO_2)$ was found by multiplying the dose rate in roentgens by 0.85. The dose to the samples was also checked with CaF_2 thermoluminescent dosimeters (TLD's). The dose rates for the ARACOR were adjusted to match the dose rates for the ^{60}Co source: 1.14 $krad(SiO_2)$/min for low total-dose irradiations (<50 $krad(SiO_2)$), and 16.74 $krad(SiO_2)$/min for high total-dose irradiations (≥50 $krad(SiO_2)$). The ^{60}Co irradiations were performed with a lead-aluminum shield (0.063 in. Pb and 0.030 in. Al) to filter out any low-energy component from scattering within the pool [16].

Figure 7 shows the threshold voltage shift for ^{60}Co and 10-keV x-ray irradiation versus dose (Fig. 7A) and charge generation (Fig. 7B) for a 500-nm field oxide MOSFET irradiated with oxide fields of 0.1 and 0.5 MV/cm. Figure 7A shows the data uncorrected for dose enhancement or fractional charge yield. The ^{60}Co data show a much larger threshold voltage shift (1.5 to 2.0 times) than do the 10-keV x-ray data at the same dose and at both 0.1 and 0.5 MV/cm. Figure 7B shows the data corrected for R_{de} and f_y with the use of the results of the previous section. The correlation was obtained by changing the abscissa from dose to charge generation ($D_o \times R_{de} \times f_y$). Plotted in this fashion, the threshold voltage shift is dependent on the free electron-hole pair density and independent of the type of radiation producing the free carriers. There is excellent agreement between the threshold voltage shifts as a function of charge generation for the ^{60}Co and 10-keV x-rays at both 0.1- and 0.5-MV/cm fields. Note that even though the 0.1- and 0.5-MV/cm curves diverge above 1×10^{-3} C/cm^3, the x-ray and ^{60}Co results remain in agreement at each field. (The divergence with field is due to charge saturation effects in the oxide at 0.1 MV/cm when ΔV_t exceeds the applied bias.)

Figure 8 shows the threshold voltage shift for ^{60}Co and 10-keV x-ray irradiation versus dose and charge generation for 40-nm gate-oxide MOSFET's irradiated with a 1.25-MV/cm oxide field. Figure 8A shows the uncorrected data and figure 8B shows the data corrected for charge generation. Although there is good correlation before the data are adjusted, this result is fortuitous. The charge generation for a 40-nm sample irradiated at 1.25 MV/cm with 10-keV x rays is almost identical in the ^{60}Co source simply because the variances in f_y and R_{de} in the x ray with respect to the ^{60}Co values almost cancel. Unfortunately, this fortuitous correlation for typical gate-oxide thicknesses and operating fields has generated the impression that dose enhancement and charge generation differences in the 10-keV x-ray and ^{60}Co environments may safely be ignored.

4. Implications for Device Testing

The results of this work clearly show that there are differences between the ionizing radiation damage produced in MOS devices by ^{60}Co and 10-keV x rays. Since ^{60}Co is usually considered the de facto standard for ionizing radiation damage, we feel the results obtained for the 10-keV x rays should be adjusted for comparison to ^{60}Co, and propose that the 10-keV x-ray results should be presented as ^{60}Co equivalent dose. That is, the dose in the 10-keV x-ray machine should be adjusted for dose enhancement and hole yield (i.e., charge generation) differences between the two sources. This correction can be arrived at by simply equating the charge generation in the two sources and obtaining the following expression:

$$D_o^{Co-60} = \frac{K_g^{x-ray} \, f_y^{x-ray} \, R_{de}^{x-ray}}{K_g^{Co-60} \, f_y^{Co-60} \, R_{de}^{Co-60}} \, D_o^{x-ray} ,$$

where $K_g^{x-ray} = 1.4 \times 10^{-6}$ C/cm^{3}rad(SiO$_2$),

$K_g^{Co-60} = 1.3 \times 10^{-6}$ C/cm^{3}rad(SiO$_2$),

f_y^{Co-60} and f_y^{x-ray} are the fractional hole yields in the ^{60}Co and 10-keV x-ray sources, and R_{de}^{Co-60} and R_{de}^{x-ray} are the dose enhancement in the ^{60}Co and 10-keV x-ray sources. R_{de}^{Co-60} is usually assumed to be 1; however some ^{60}Co sources can have an appreciable low-energy component [16]. D_o^{x-ray} is the bulk dose (independent of dose enhancement) in rad(SiO$_2$) in the x-ray machine, and D_o^{Co-60} is the ^{60}Co equivalent dose in rad(SiO$_2$).

All the terms in the above expression can be easily obtained from existing data in the literature (e.g., the present work), providing the oxide thickness and applied bias during irradiation are known. This makes the ^{60}Co equivalent dose correction well suited to individual device, test structure, or simple circuit testing, since the oxide thickness and fields are usually known. However, the x-ray/^{60}Co dose correction is not as easily applied to failure level testing of complex circuits. In most cases the oxide thicknesses and operating fields are not known, so the dose enhancement and fractional hole yield differences cannot be properly adjusted (although reasonable values can usually be obtained). Also, no one adjustment can match x-ray and ^{60}Co charge generation (and, hence, damage) in gate- and field-oxide structures at the same time. (But this is always true, whether or not this technique is used. This difference might even be exploited to determine device failure mode.) Pass/fail testing of complex circuits in the low-energy x-ray environment has another implication if the results are to be interpreted correctly. If the failure mechanisms cannot be readily identified (i.e., gate-oxide-induced threshold voltage shift or field-oxide-induced leakage currents), calculations of ^{60}Co-equivalent dose need to be made for both the gate and field oxides using best estimates for oxide thickness and fields. Then the ^{60}Co-equivalent dose to failure must, for safety, be assumed to be the lesser of the two calculated doses.

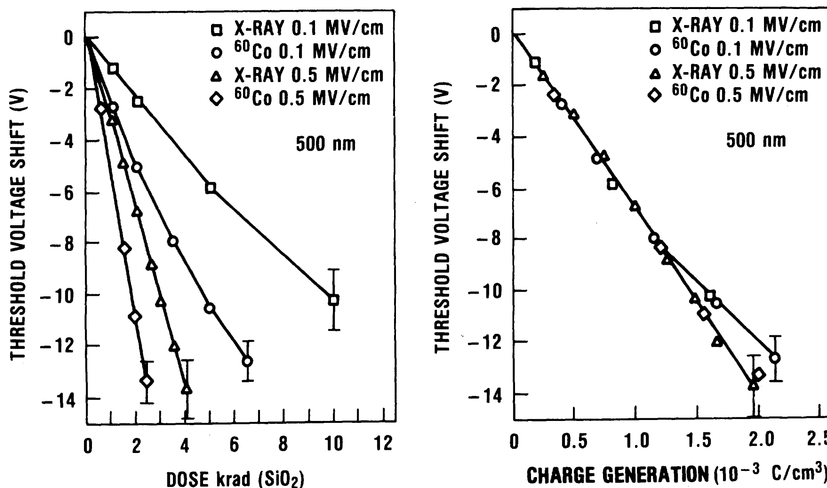

Figure 7. Threshold voltage correlation for 500-nm field oxide MOSFET's irradiated in ^{60}CO and 10-keV x rays at 0.1 and 0.5 MV/cm. Figure 7A is threshold voltage shift versus dose (uncorrected for R_{de}). Figure 7B is threshold voltage shift plotted versus charge generation.

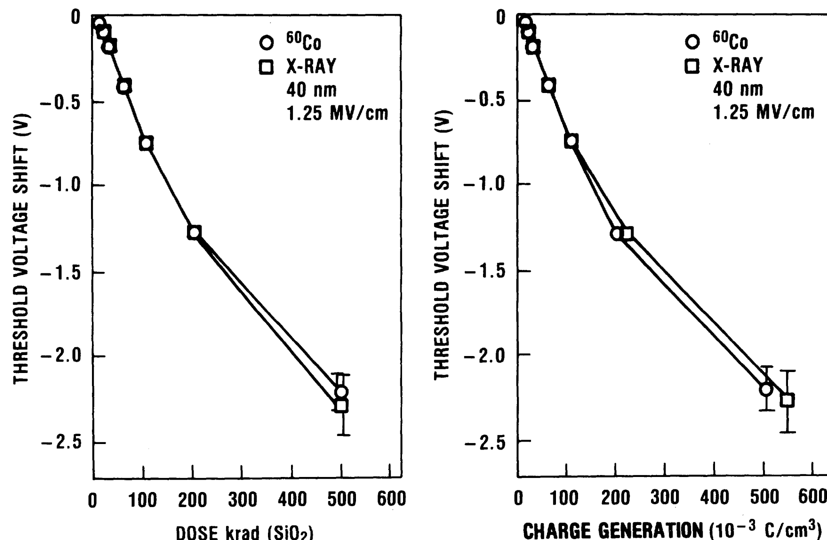

Figure 8. Threshold voltage correlation for 40-nm gate-oxide MOSFET's irradiated in ^{60}Co and 10-keV x rays at 1.25 MV/cm. Figure 8A is the threshold voltage shift versus bulk dose (uncorrected for R_{de}). Figure 8B is the threshold voltage shift plotted versus charge generation.

5. Summary/Conclusions

We have employed a conduction current measurement to independently measure the fractional charge yield and dose enhancement in a 10-keV x-ray environment. We applied the charge yield and dose enhancement results in turn to correlate the threshold voltage shifts in gate- and field-oxide MOSFET's irradiated with ^{60}Co and 10-keV x rays. The correlation was obtained by using the radiation-generated charge density (charge generation) as a measure of the oxide damage instead of dose. The correlation worked well for all the samples tested, which included a 40-nm gate-oxide MOSFET irradiated at 1.25 MV/cm and a 500-nm field-oxide MOSFET irradiated with oxide fields of 0.1 and 0.5 MV/cm. We presented a procedure for adjusting the dose from a 10-keV x-ray machine for dose enhancement and hole yield to obtain the equivalent ^{60}Co dose for devices for which the oxide thickness and fields are known. Finally, we discussed the implications of using low-energy x rays for device testing and qualification.

6. References

1. C. M. Dozier, D. B. Brown, J. L. Throckmorton, and D. I. Ma, "Defect Production in SiO_2 by X-ray and ^{60}Co Radiations," IEEE Trans. Nucl. Sci. NS-32, No. 6, 4363-4368 (1985).

2. C. M. Dozier and D. B. Brown, "The Use of Low Energy X-Rays for Device Testing--A Comparison with ^{60}Co Radiation," IEEE Trans. Nucl. Sci. NS-30, No. 6, 4382-4387 (1983).

3. C. M. Dozier and D. B. Brown, "The Effect of Photon Energy on the Response of MOS Devices," IEEE Trans. Nucl. Sci. NS-28, No. 6, 4137-4141 (1981).

4. C. M. Dozier and D. B. Brown, "Photon Energy Dependence of Radiation Effects in MOS Structures," IEEE Trans. Nucl. Sci. NS-27, No. 6, 1694-1699 (1980).

5. T. R. Oldham and J. M. McGarrity, "Comparison of ^{60}Co Response and 10 keV X-ray Response in MOS Capacitors," IEEE Trans. Nucl. Sci. NS-30, No. 6, 4377-4381 (1983).

6. H. E. Boesch, Jr., "Hole Transport and Trapping in Field Oxides," IEEE Trans. Nucl. Sci. NS-32, No. 6, 3940-3945 (1985).

7. D. B. Brown, "The Time Dependence of Interface State Production," IEEE Trans. Nucl. Sci. NS-32, No. 6, 3900-3904 (1985).

8. D. L. Griscom, "Diffusion of Radiolytic Molecular Hydrogen as a Mechanism for the Post-Irradiation Buildup of Interface States in SiO_2-on-Si Structures," J. Appl. Phys. 58, 2524 (1985).

9. F. B. McLean, "Interface States in SiO_2 MOS Structures," IEEE Trans. Nucl. Sci. NS-27, No. 6, 1651-1657 (1980).

10. D. B. Brown, "Photoelectron Effects on the Dose Deposited in MOS Devices by Low Energy X-ray Sources," IEEE Trans. Nucl. Sci. NS-27, No. 6, 1465-1468 (1980).

11. G. A. Ausman, Jr., and F. B. McLean, "Electron-Hole Pair Creation Energy in SiO_2," Appl. Phys. Lett. 26 173-175 (1975).

12. D. B. Brown, "The Phenomenon of Electron Rollout for Energy Deposition in MOS Devices," to be published, IEEE Trans. Nucl. Sci. (Dec. 1986).

13. D. B. Brown, private communication.

14. H. E. Boesch, Jr. and J. M. McGarrity, "Charge Yield and Dose Effects in MOS Capacitors at 80 K," IEEE Trans. Nucl. Sci. NS-23, No. 6, 1520-1525 (1976).

15. F. Briggs and R. Lighthill, "Analytical Approximations for X-ray Cross Sections 11," Sandia Laboratories Technical Report, SC-RR-71-0507 (1971).

16. K. G. Kerris and S. G. Gorbics, "Experimental Determination of the Low-Energy Spectral Component of Cobalt-60 Sources," IEEE Trans. Nucl. Sci. NS-32, No. 6, 4356-4362 (1985).